Solid Freeform Fabrication 2017: Proceedings of the 28th Annual International
Solid Freeform Fabrication Symposium – An Additive Manufacturing Conference
Reviewed Paper

IN SITU MELT POOL MONITORING AND THE CORRELATION TO PART DENSITY OF INCONEL® 718 FOR QUALITY ASSURANCE IN SELECTIVE LASER MELTING

D. Alberts[1], D. Schwarze[1], G. Witt[2]

SLM Solutions Group AG, Roggenhorster Straße 9c, 23556 Lübeck, Germany
University of Duisburg-Essen, Institute for Product Engineering, Chair of Manufacturing Technology, Lotharstraße 1, 47057 Duisburg, Germany

Abstract

Additive Manufacturing looks back on a history of about two decades and today SLM® technology keeps moving as an integral element in industrial production environments. Sensitive markets such as energy, medical or aerospace have the highest quality standards for complex, safety-related and highly stressed components which are to be met at competitive costs for each build job and single part. In this context process monitoring is necessary for documentation, qualification and at the same time it is expected to be able to detect process anomalies during the process. In addition to surface roughness, part density which mostly depends on volume energy, changing with laser power, scan velocity etc., is a distinctive quality feature of every component. This paper presents a method for a real time melt pool monitoring system based on photodiodes and the correlation between thermal emission and part density of Inconel® 718 with respect to volume energy deviation.

Keywords: In situ; real time; melt pool monitoring; Selective Laser Melting; part density; Inconel® 718.

Introduction

Over the last twenty-five years, Additive Manufacturing (AM) has established itself beside conventional manufacturing technologies in industrial production environments. It is now possible to use AM for small-batch manufacturing or even quantity production with good productivity, repeatability and reliability.

With respect to productivity, multi-laser or rather multi-optic SLM® technology is available with up to four simultaneously working laser sources on one part or multiple parts in one layer for a whole build job [WS14]. Moreover, laser power is being continuously increased to higher power, with up to 1000 W now available, and different kind of beam profiles available to increase build rates [BSH11, SLM17].

One of the biggest advantages of AM due to geometrical freedom is the capability to create special and complex elements like lattice or honeycomb structures as well as overhangs or undercuts [Reh10]. Selected parts have the potential due to a redesign to implement lightweight structures as well as optimized fluid properties or stress reduction [RAH13, YHC16]. On one hand, there is the capability to integrate a number of separate parts in a single unit and to eliminate further process iterations. On the other hand, there are other selected examples of reducing production steps by substituting conventional technologies with SLM® technology for example in existing repair applications [Sch14, Kro15].

In addition to be able to produce nearly fully dense metal materials, mechanical properties can be comparable to conventional wrought or cast metals. However, multiple process parameters, machines and environmental conditions can make it challenging to achieve repeatability in the final part quality. Significant time and cost is invested in non-destructive testing to analyses part quality and to ensure the quality requirements of the final component.

Motivation

Besides the quality check of a final component after the job as part of post-processing it is required to reach further process understanding being able to follow the job results down to single part behavior. Process monitoring systems in the AM environment should have the capability to detect process anomalies, as well as provide a documented record of the entire process for traceability. The overall motivation is establishing a

method to correlate signal or ratio response of process monitoring systems during the job and tracing them back to build part quality. The goal is to differentiate afterwards (offline) or even during the build (online) between components, determining which reach their quality threshold and which not. An offline pass/fail job report would reduce time and cost for post-processing. Part-related real time monitoring and online detection of failed parts, which could be deleted from the current job, leads directly to a fabrication time reduction. However, the procedure should end up with more stable part quality, reduction or prevention of quality variations and ensuring the reproducibility of ready-to-use AM parts [WPH14, Alb16, WSP14].

State of the art

Industry and science are focusing on the development, application and usage of monitoring systems, which can divided due to the observation of laser or primary emissions as well as secondary emissions. Observation of secondary emissions means from the process emitted thermal emissions, imaging, ultrasound, low coherence interferometry (LCI) or acoustic procedures. Furthermore, we can distinguish between sensor layouts of off-axis or on-axis systems.

One of the first approaches used acoustic measurement, which is based on measuring the surface acoustic wave velocity. Smith et.al presented comparable results by electron microscopy and x-ray computed tomography relating to defect measurement like pores and roughness by changing the laser power between 70 W up to 200 W [SHP16]. There is actually no applied system directly to SLM technology but it look like a promising and visible possibility due to off-axis or on-axis observation in the future.

Neef et al. integrated an on-axis sensor setup in a SLM® machine based on LCI. The system is able to measure topology part information during and between the recoating procedures in which anomalies based on the relation of powder and SLM® structures has been shown. [Nee14]

Rieder et al. was using ultrasonic as an off-axis online as well as an offline inspection for test specimens out of Inconel® 718. Due to the online monitoring procedure and comparison of a CT-image the correlation of ultrasonic signals and the microstructure behavior with respect to laser power variations were shown [RSB16].

Off-axis imaging is mostly and already commercial available to detect insufficient powder recoating [KAS15]. There can be an image documentation after powder application as well as after exposure. Based on an automatic analysis of the captured image an error detection is implemented with respect to manual adjustment of conditions and error detection limits. It supports immediately individual process errors due to powder supply and it controls post coating procedure. More in detail, Kleszczynski et al. presents a high-resolution CCD camera to evaluate solidified scan pattern after powder application layer by layer [KZS12]. By means of the resulting layer topography, variations of volume energy are detectable and recoating errors were visualized based on overhang structures [KZS14].

Another image-based off-axis process monitoring approach has been developed by Krauss using thermography. Krauss differs in his research between global inspection, layer-based inspection and local inspection (layer resolved observation). Via generating indicators, an adjusted analysis was used to create a performance measurement system, which enabled quality evaluation. His research focuses on system resolution, ability of detection and temperature determination. Different kinds of process phenomena were carried out which could correlate to build part quality. [Kra17]

Other on-axis approaches used to extract thermal emissions via photodiodes. Pavlov et al. use an f-theta lens as focusing unit and two photodiodes which are sensitive in the dedicate wavelengths of 1200 nm and 1400 nm. The relation between signal response and variations of layer thickness as well as hatch distance were shown with respect to single scan vectors. Afterwards, different scan strategies were used on test samples to analyze signal fluctuations and their correlation to melt pool instability. [PDS10]

Berumen et al. describe an f-theta machine setup equipped with one photodiode and a spectral range of 780 nm up to 900 nm. Overhang structures, sharp contours as well as unplanned layer thickness variations were identified by means of process errors during the delivery of the build platform. Due to heat accumulation, a correlation to part defects could be demonstrated for all three experiments with respect to photodiodes and their combination with a high-speed camera. [BBL10]

Spears et al. were able to draw a fundamental relation between a resulting energy density via laser power variations as well as the correlation between the signal profile and the porosity. The machine setup as well as material and process parameters were not specified. [SG16]

Objective

Surface roughness, hardness and part density are well-defined as distinctive global part quality features. Especially part density results of the sum with respect to part defects like pores, cracks, shrinkages etc. and leads to mechanical properties. The Key Process Variables (KPVs) that affect the density of parts produced by the Selective Laser Melting process are laser power, scan velocity, hatch distance and layer thickness. These KPVs can be used to describe the "volume energy", i.e. the total energy input into the component, in units of J/mm^3. The target of this study is to show the correlation between thermal emission response, volume energy variation and final part density with a photodiode-based in situ melt pool monitoring system to enable the system to use as an online/offline quality assurance method for Selective Laser Melting.

In this work, we investigate the photodiode response by changing the wall energy or volume energy for single as well as multiple scan vectors. Also, we assessed whether the part density correlates with the monitoring data. It is also an objective to analyze if the system is sensitive for process parameter change and if they are able to distinguish from each other.

Experimental setup

Machine and Optical System

The in situ process monitoring system to be developed requires the possibility of integration and usage in established manufacturing systems of SLM Solutions. In addition, the systems are designed to work regardless of machine sizes and machine types, e.g. multi-laser / multi-scanner systems and the kW power range. Figure 1 (a) shows an SLM280 system from SLM Solutions and the optic design of a modular-built manufacturing system as a part of the whole machine concept is shown schematically in Figure 1 (b).

The fiber tip of a diode-pumped single-mode CW fiber laser is coupled into a collimation unit, which is adjusted for the particular machine system. The collimated beam aligns axially to a 3D focusing unit, which allows a highly dynamic and high-precision positioning of laser focus along the optical axis. This unit is optimized for applications with high power densities in particular and replaces elaborate flat-field objectives. A scan system with digital control electronics and customized coating is used for high-precision positioning and deflection of the process beam to the particular process plane.

The process radiation occurring from the exposure of several vector types and locally welded powder particles is a thermal emission signal, which diffusely emits from the melt pool. It is utilized as input value of the melt pool monitoring device. Beam splitter 1, shown in Figure 1 (b), reflects thermal emissions at the rear surface seen from direction of the fiber, which reflect back along the optical axis into the opposite direction of the beam path. The upwards reflect wave lengths from primary optical axis is aligned vertically to the optical buildup of the melt pool monitoring device in which it will reflect on a further mirror through a focusing lens. Finally, beam splitter 2 splits the signals for photodiode 1 and photodiode 2.

The front surface of beam splitter 1 transmits the laser wavelength and a proportion of the reflection serves as an input signal for photodiode 3 for a laser power monitoring device.

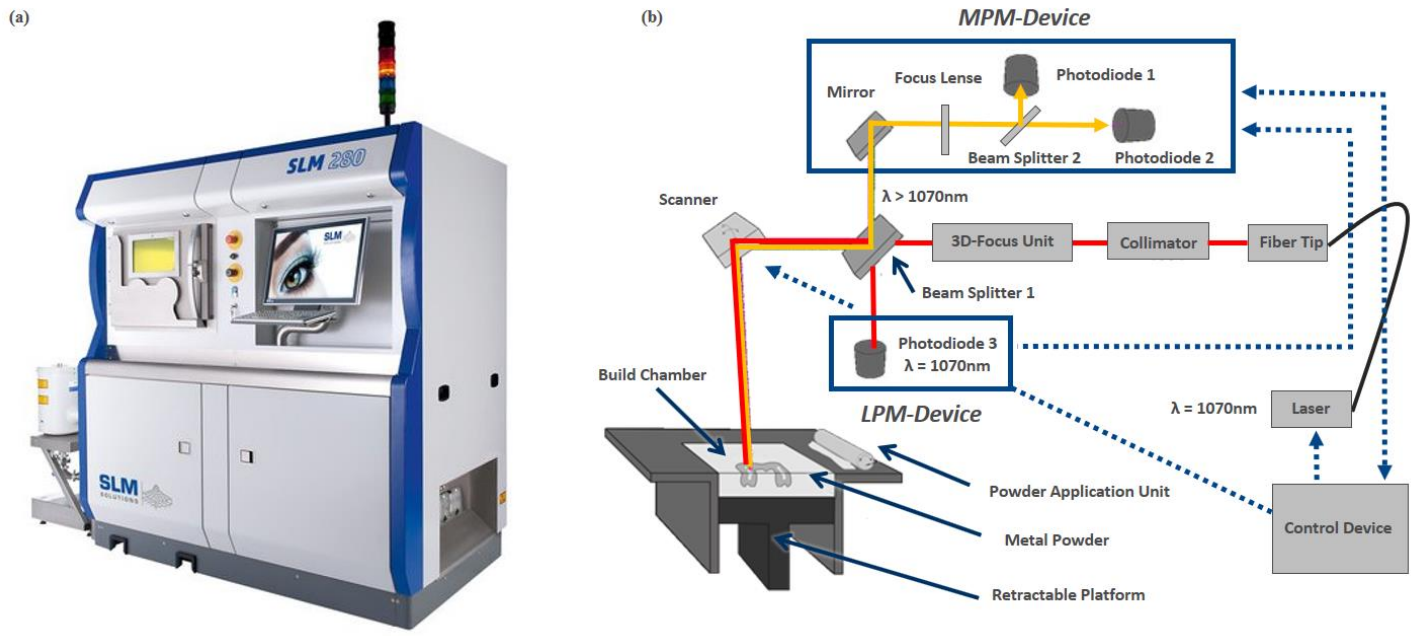

Figure 1: (a) SLM 280; (b) Schematic assembly of optic design with melt pool monitoring and laser power monitoring.

Melt Pool Monitoring and Laser Power Monitoring System

The melt pool monitoring system uses two photodiodes with different dedicated photosensitivity as a function of wavelengths – each is detecting near-infrared wavelengths, but the wavelength detected by ADC1 is different than the wavelength detected by ADC2. Spectral response is permanently taken up by the individual photodiodes, forwarded to an ADC (analog digital converter) and provided in an FPGA (field programmable gate array). ADC1 is associated to photodiode 1 and ADC2 is associated to photodiode 2. Depending on machine and optical system setup as well as taking into account two different photodiodes the signal-to-noise ratio is at present up to 10.

As described the reflected portion of the laser wavelength via beam splitter 1 is used as an input signal (measured laser power) of the present laser power (set laser power) by means of photodiode 3. The consumed electric current is converted into an electrical voltage and provided every 100 kHz via ADC1 and ADC2. The measured laser power is then transferred from the LPM device to the MPM device. In addition to [ASW16] the two process monitoring systems are combined and both of them are directly linked to x/y-coordinates which is provided by an interface of the control device.

Thermal emissions, the laser-on/off signal, the set laser power and the measured laser power is combined to the present x/y-coordinates (16-bit) as well as is provided from the FPGA to the control device every 10 µs. The FPGA controls the correct timing of the input signals, other potential operations and the subsequent measurement task of 10 µs. All data packages of a measurement task are stored every layer in a data file and can be traced back clearly due to time function and are able to read out. After completion of the exposure of a layer, a new file is created automatically. During the process the output is represented in the form of a live 2D representation of the whole build platform, see figure 2 (a). The associated raw signals of a selected scan vector are shown in figure 2 (b).

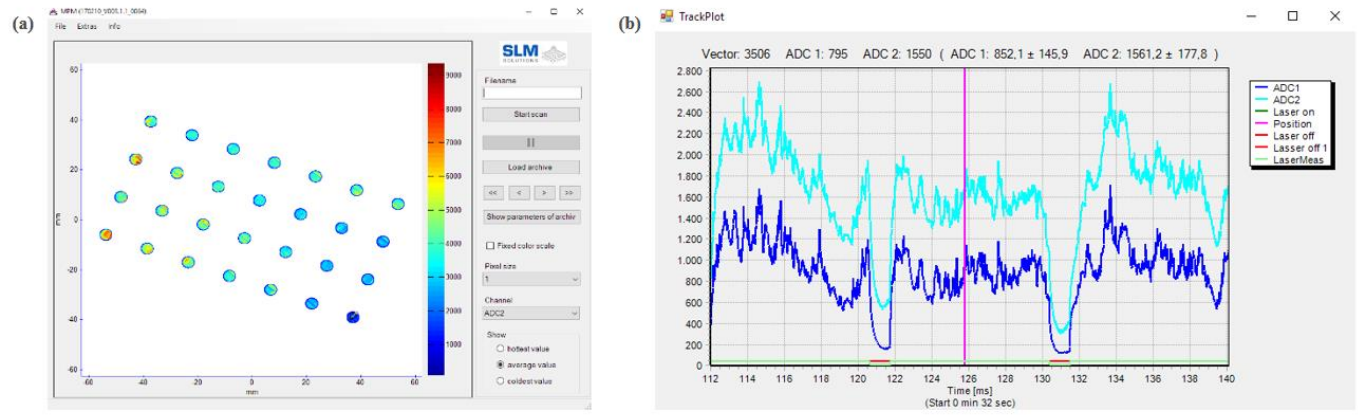

Figure 2: (a) 2D representation of thermal emissions (b) and complementary "Track Plot" of selected scan vectors.

Experimental description, results and discussion

The following section describes three experiments, which build upon one another. Each experiment contains a description, procedure, results and discussion, which is evaluated independently from each other. Based on the following parameter variations with respect to laser power (P_L), layer thickness (D_L), scan velocity (V_S) and hatch distance (d_T) the following energy calculations for the experiments can be made.

$$E_W = \frac{P_L}{D_L \times V_S} [J/mm^2] \quad (1) \qquad E_V = \frac{P_L}{D_L \times V_S \times d_T} [J/mm^3] \quad (2)$$

The energy of the single scan vector approach can be defined as the energy input of a wall, E_W, respectively a contour or a first track of a hatch pattern shown in equation (1). The basis for calculating the energy of a volume shown in equation (2). E_V is used to describe multiple scan vector within the single scan vector approach with respect to hatch distance as well as the volume of test specimens.

An already developed, proved and validated material file of Inconel® 718 serves as a basis for the following experiments. Standardized wall and volume energies are used in which energy "1" belongs to the developed parameter set and results in average part density of 99,8 % which based on 50 µm layer thickness. The possibility to build high quality parts under controlled conditions is a basis requirement before changing various influencing parameters and conditions and use them for further data approaches and correlation to various indicators.

Basis intensity behavior of different process and measuring situations

The sum of single measurement points with respect to the MPM device is relating to a single layer information shown in Figure 3 (a). Single test sample or build parts result on one hand to constant process parameters, like scan velocity etc., for specific scan vector types, for example support structures, contours or hatch areas. On the other hand, there are clearly defined but variable process parameters, like rotation scan strategies or scanning sequences. These parameters rely in combination to machine environment and process conditions as well as positioning of part to different process and measurement situations for the MPM device. It is the aim to make different situations visible via comparing photodiode response when each photodiode is accurate adjusted to the current laser position.

Although the process parameters for any given scan vector may be nominally identical, there may be a significant difference in the emission detected by the Melt Pool Monitor due to the prior conditions of the local area being scanned. A distinction is made between "No Exposure" situation, means detection of powder material, Figure 3 (b), as well as the measuring situation of a first single scan vector without any other neighboring solidified scan vectors in the detection area, "Track 1" Figure 3 (c), which can represents a contour track.

Furthermore, there is the situation of a second scan track surrounded by powder material due to the MPM detection area, “Track 2” Figure 3 (d), in which one single scan vector will be expose next to the first solidified scan vector on a certain distance. Next situation, see “Track n+1” Figure 3 (e), represents for example a hatch exposure. The MPM device is detecting the emitted thermal emissions of a single scan vector, which is positioned next to multiple and solidified single scan vectors in the first half of the detection area. Multiple scan vectors are exposed immediately after each other. The second half of the detection area is covered with powder. The last process situation, “Track 2n+1” Figure 3 (f), represents a single scan vector surrounded by solidified scan vectors on both sides of the current measurement point in the detection area.

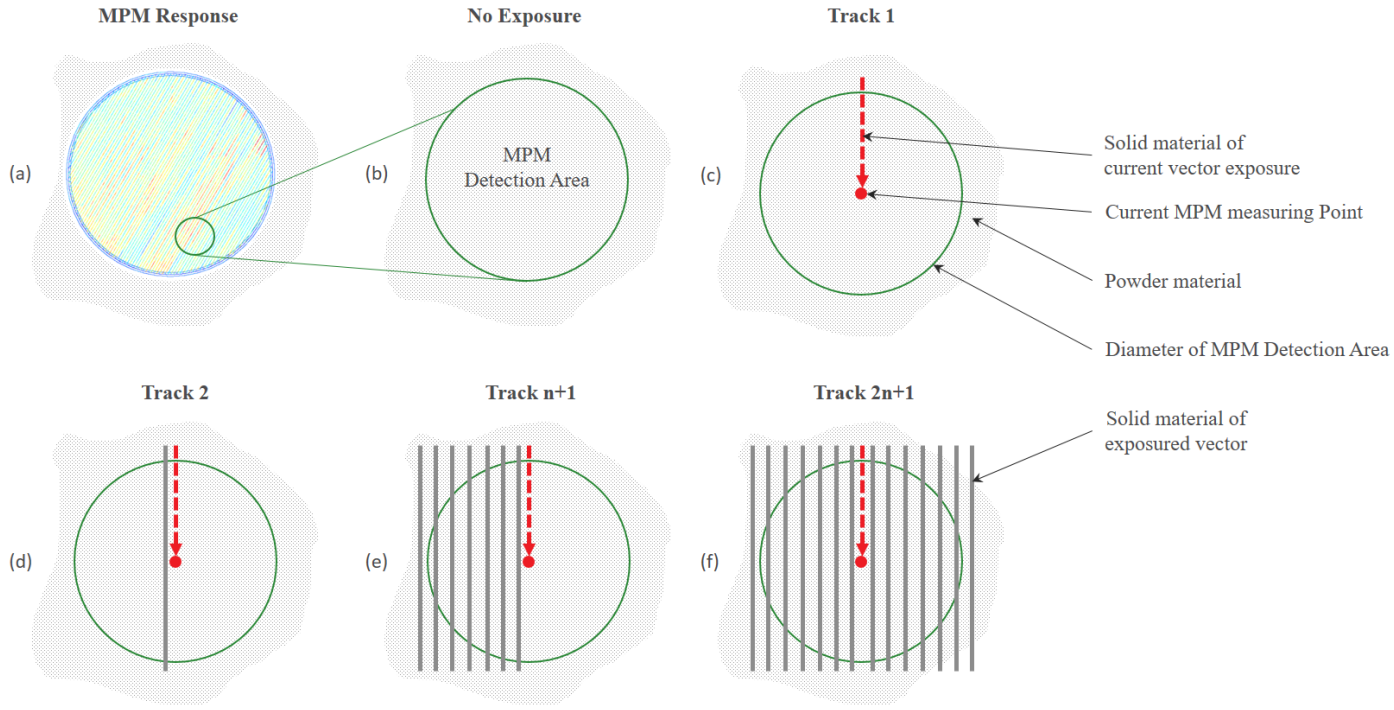

Figure 3: Basis intensity behavior of different process and measuring situations.

For the current approach, single scan vectors were exposed on the first layer of a base plate with a standardized wall energy due to layer thickness, laser power and scan velocity variations. With respect to hatch distance variations a standardized volume energy is used. Single scan vectors are exposed in the opposite direction of the laminar gas flow in the build chamber. For statistic validation, each process and measuring situation is repeated five times, so the results illustrate the average value as well as standard deviation of thermal emissions. The averaged value for every single scan vector is determined via automatically read out from the “Track Plot”, Figure 2 (b), of the MPM device, which has a measurement rate of 10 µs.

Figure 4 shows a continuous decrease of photodiode response with respect to thermal emissions due to “Track 1”, “Track 2”, “Track n+1” and “Track 2n+1” independent of ADC1 and ADC2. The lower level of thermal emission response of about 5 % to 18 % in between each situation base on different conditions regarding to the current heat conduction situation. The surrounded powder of the “Track 1” approach acts as an isolator and leads the entered energy for heat dissipation limited to the base plate. During the “Track 2” approach, entered energy can additionally dissipate because of the neighboring scan vector. Even when there are already certain single scan vectors are placed next to each other, heat dissipation is apparently going on so rapidly that residual heat from neighboring scan vectors are not influencing the result during “Track n+1” as well as “Track 2n+1” approach. For every approach, thermal emission response for ADC2 is consistently 10 % to 14 % higher than ADC1. Standard deviations of ADC2 compare to ADC1 are in the first two approaches 21 % to 23 % higher than in the “Track n+1” or “Track 2n+1” approach. Within the two last approaches, standard deviations of ADC1 are 13 % to 18 % higher than ADC2. One of the reasons for this fact could be a smaller number of spatters or ejected powder, which were recognized and could be detected from the MPM device in the experiment.

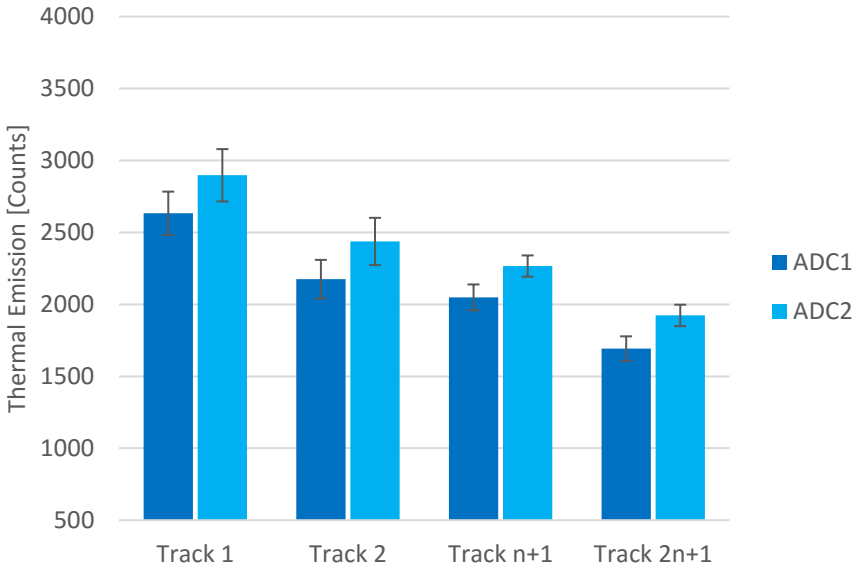

Figure 4: Basis intensity behavior of different process and measuring situations.

Single and multiple scan vectors wall and volume energies

In the next experiment, it was used the single scan vector approach and made selective variations with respect to layer thickness, laser power, scan velocity and hatch distance. The purpose was to analyze the general relation between wall energy and volume energy variations and photodiode response. The aim is to understand how different process parameters affect the MPM signals.

As with the previous experiment, single scan vectors are exposed on the first layer of a base plate. For statistic validation, each process parameter is repeated five times, so the results illustrate the average value and standard deviation of thermal emissions. The averaged value for every single scan vector is determined via automatically read out from the "Track Plot" of the MPM device, which has a measurement rate of 10 µs.

Energy variations with respect to layer thickness, laser power and scan velocity changes, lead to a standardized wall energy change as well as hatch distance changes to a standardized volume energy change. Beside the standard parameter "1", there are six additional energy levels for each parameter, which change ±15 % up to maximum variations of ± 45 %. Contrary to all other experiments, six application-oriented layer thicknesses are selected which correspond to a wall energy range of – 83 % to + 150 % compared to the standard parameter. Being able to produce all single scan vectors in one job, 10 mm long grooves relating to the selected layer thicknesses were milled into the base plate before.

In Figure 5, photodiode response with respect to thermal emissions of ADC1 and ADC2 are shown over standardized wall energies due to layer thickness variations. The experiment simply increased or decreased the layer thickness from the standard value, and is presented in terms of the resulting wall energy, see equation 1. Increasing wall energy because of smaller layer thickness results in a decreasing photodiode response. With thinner layers (higher wall energy), heat is able to be conducted away quickly to the base plate, thus the thermal emission is reduced. The results can be divided into three sectors. Within a wall energy variation between "1" up to "2,50" no significant variation of thermal emissions can be noticed. From a lower limit of the layer thickness a balanced heat dissipation is given. Between "1" up to "0,33" there is a constant and almost linear increase of ADC1 and ADC2 which shows the range of measurement sensitivity. Within that range, wall energy changes correlates with photodiode response due to layer thickness variations. Sector three, between "0,33" up to "0,17" there is an almost constant photodiode response. From an upper limit of the layer thickness, the resulting powder quantity is insignificant, since only a small or no connection to the layer below or base plate exists.

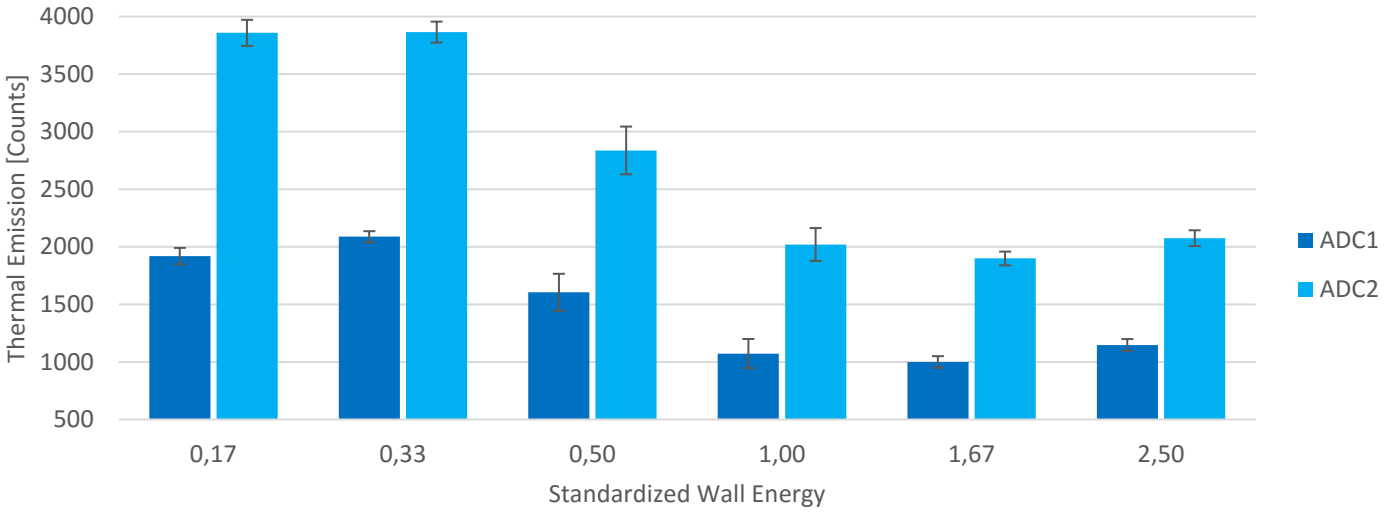

Figure 5: Thermal emissions response over standardized wall energies due to different layer thicknesses.

Figure 6 shows thermal emissions of ADC1, Figure 6 left, and ADC2, Figure 6 right, over wall energy variations by changing laser power and scan velocity as well as volume energy variations by changing hatch distance. Average thermal emissions as well as standard deviation for each process parameter and their specific variation up to ±45 % shows same dimensions for ADC1 and ADC2 and can be used for evaluating the single and multiple scan vector approach at the same time.

Laser power and scan velocity approach is linked to the "Track 1" experiment as well as hatch distance to the "Track n+1" experiment, shown in the prior approach "Basis intensity behavior of different process and measuring situations".

Thermal emission response of laser power and scan velocity variations correlates significantly with increasing wall energy. Despite identical wall and volume energy variations, there is a process-parameter-dependent photodiode response in which at lower wall and volume energy of 55 % with respect to the standard parameter "1" scan velocity and hatch distance is almost at the response level. By energy increase there is a change of thermal emission response for laser power and scan velocity with an intersection at the standard parameter, which could allow a determination between process parameters due to thermal emission response.

In this experimental procedure, hatch distance variations have actually no effect on thermal emission response, even not on a wide range of volume energy variation. One explanation could be within the single respectively multiple scan vector approach, that there is a direct heat conduction to the base plate. This procedure does not represent the fabrication process of a real part in which there is normally, depending on part dimension, not a comparable heat conduction as shown here. However, correlation between hatch distance and the global quality feature of density is state of the art and the correlation to photodiode response should be checked on test specimens once again.

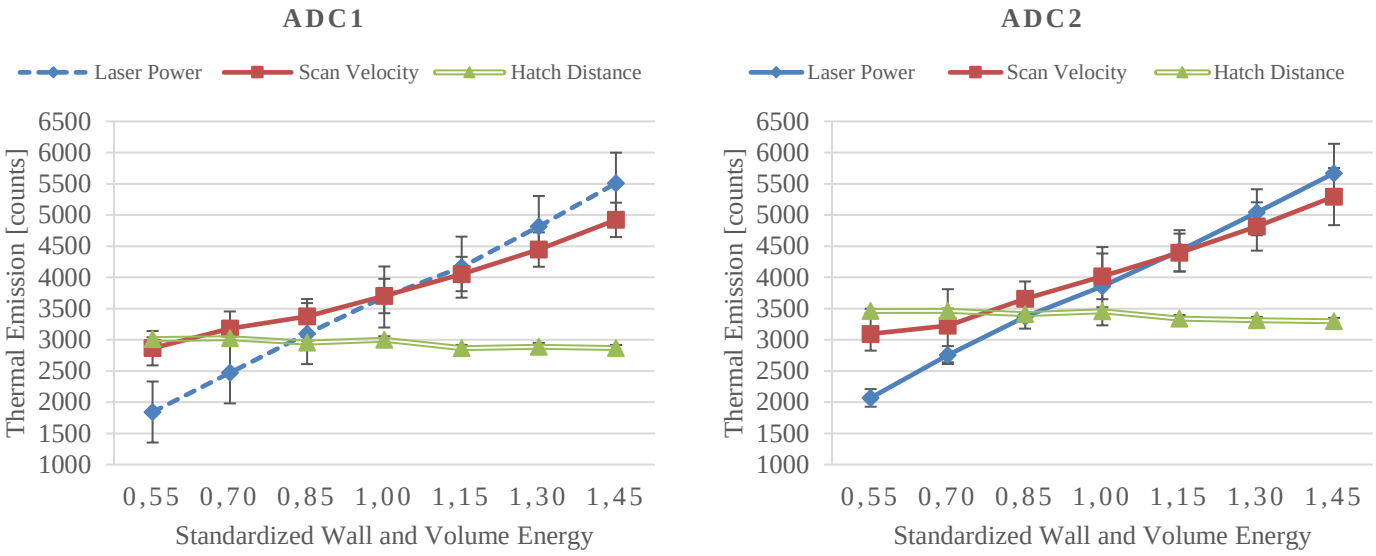

Figure 6: Thermal emissions response of single and multiple scan vectors over standardized wall and volume energies due to laser power, scan velocity and hatch distance variations.

Correlation between photodiode response and part density

In this third experiment, cylinders each with a height of 10 mm and 10 mm diameter, were produced in three different jobs as shown in Figure 7. In the first two jobs the layer thickness was varied. In the third job, laser power, scan velocity and hatch distance were varied as shown at the bottom right in Figure 7.

The first job was built with nine specimens for each layer thickness, starting with 40 µm. Afterwards, the next nine cylinders with a layer thickness of 30 µm was built on the same position and on top of the first existing specimens. The final nine cylinders had a layer thickness of 20 µm. The second job follows the same procedure as the first job with a layer thickness variation of 50 µm, 100 µm and 150 µm. Test specimens of the third job, based on 50 µm layer thickness, were built by changing volume energy in steps of 15 % each to a maximum of ±45 %. In fact, there are fifty-four specimens due to layer thickness variation and seven specimens each for laser power, scan velocity and hatch distance variations.

For the current approach the MPM device had a measurement rate of 10 µs, which means a parameter depending quantity of measurement points between 5,6 million and 72,8 million per specimen. The averaged value as well as standard deviation for every specimen is determined within a big data approach using computer language of Python.

Density testing was performed for every specimen by doing metallographic studies via cutting, embedding, grinding, polishing and finally using standard software for density detection with light microscopy.

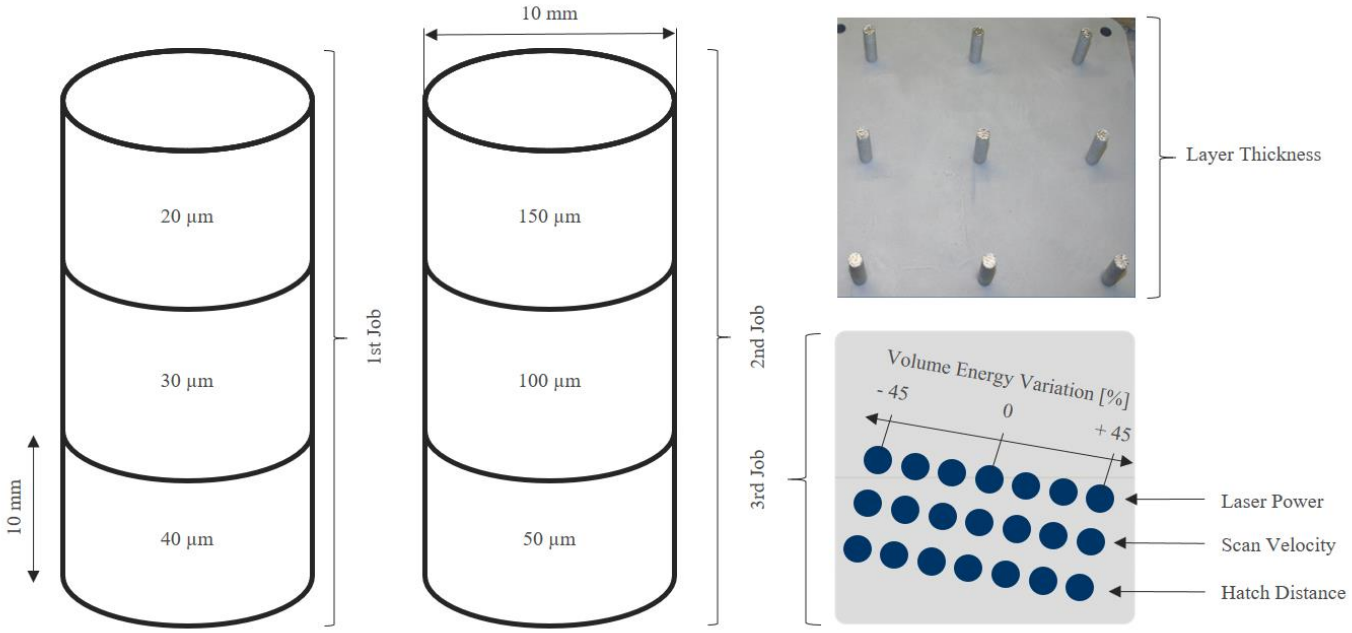

Figure 7: Jobs and test specimens for process parameter variations.

The results for the experiment, correlation between part density and photodiode response over volume energy with respect to variation of certain process parameter, can be seen in Figure 8 and Figure 9. The representation contains four process parameter variations with respect to layer thickness, laser power, scan velocity and hatch distance.

Standardized volume energy "1" belongs to the standard parameter set as already mentioned and results in average part density of 99,8 % during the three jobs. Increases in volume energy above "1" also results in dense parts. There are significant hot spots observed during manufacture of the specimens, which occur to higher surface roughness due to qualitative impression. This also leads to rising or decreasing thermal emission response for ADC1 and ADC2 between 10 % to 100%, depending on the process parameter.

An increase in layer thickness decreases the current volume energy, and results in lower part density. Compare to all other process parameter variations in that paper due to a separated inspection for ADC1 and ADC2, a rising thermal emission results in significantly higher deviation of response due to ADC1 and ADC2 and resulting in denser parts. Results for layer thickness variations corresponds to contrary behavior and needs a different interpretation approach. For bigger layer thicknesses, powder is isolating most of the heat and results in significant hot spots as well as a lot of ejected powder and spatters. Smaller layer thicknesses result in a high level of heat conduction and lead to very shiny surfaces. That behavior can be seen in Figure 8 (left), which correlates inversely-proportional with part density. The inspection of ADC1 and ADC2 separated from each other contain among other melt pool size as well as melt pool temperature. The quotient evaluation of ADC1 and ADC2, see Figure 8 (right), eliminates the influence of the emitted area, the emissivity of the material, and contains the emissivity-independent temperature correlation. As seen, the emitted area has a significantly higher influence on the photodiode response and acts as an exponential influence compare to an almost linear characteristic of the melt pool temperature. There it can be seen a clearly correlation between ADC1/ADC2 to part density and all results of analysis can be completely distinguish and classified from each other via a density deviation <0,1 %.

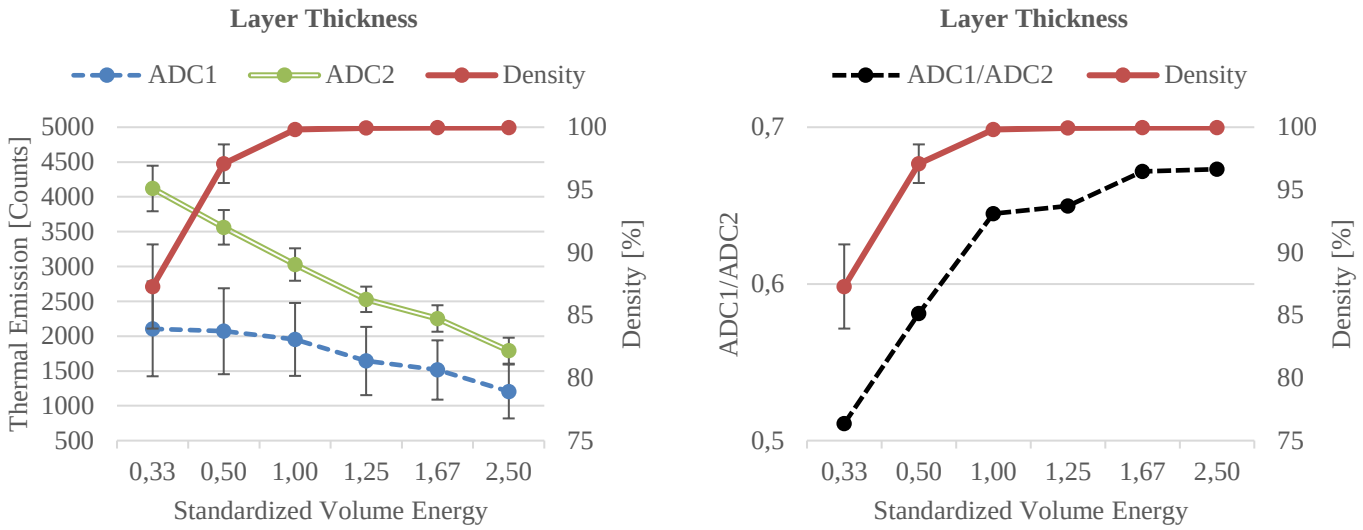

Figure 8: Correlation between photodiode response due to ADC1 and ADC2 (left) as well as ADC1/ADC2 (right) and volume energy variation via layer thickness change.

Correlation between volume energy due to laser power as well as scan velocity variations and part density shows top left and right of Figure 9. A dedicated inspection of ADC1 and ADC2, which is not shown here, indicates a close average value with respect to lower volume energy and rise up as the same time with higher volume energy. The increase of the independent photodiode response evaluation is almost linear up to a certain part density, which meets the reference volume energy level “1”. After that part density is higher than 99,7 %, the analysis of ADC1/ADC2 shows a clear correlation to part density as already shown in the layer thickness approach. Higher laser power correspond to a higher energy input per unit time and results in higher photodiode response. In this analysis, a resolution limit of the density can be specified with an accuracy of less than 0.1 %.

At the bottom left in Figure 9 the correlation between volume energy variations depending on hatch distance and part density is shown. A smaller hatch distance, which means higher volume energy, leads to a rising part density of up to >99,9 %. A minimum part density of about 99,8 % is already reached by a smaller volume energy of -15 % due to the reference parameter. Contrary to previous investigation, hatch distance or volume energy variations, does not correlates with part density without any objection. The dedicated inspection of ADC1 and ADC2 as well as ADC1/ADC2 shows the linear characteristic up to a certain point. Although the photodiode response starts to decrease, part density is increasing up to the energy volume reference of >99,9 %. Following smaller hatch distances leads to a small but continuous decrease of part density of <0,1 %. The decrease of photodiode response at a volume energy offset of +45 % is in between the results of -30 % and -45 %, which belongs to a part density below 90 %. Bigger hatch distances belong to smaller volume energy and have no conductive connection to the vector next to the current one. Like in the layer thickness approach, just on a layer-based instead of a volume-based explanation, distance of two vector paths is so big, that the emitted area is expected to grow. On the other hand, melt pool temperature is obviously not immoderately rising. Bigger hatch distances indicate poorer heat dissipation and there is a well-defined limited area of emission because of the present solid material next to the current vector. Compared to the layer thickness approach, from the beginning of a certain layer thickness the emitted area is not limited due to the layer below. On the other hand, smaller hatch distances indicate better heat dissipation but a higher amount of residual heat. These effects correspond to a photodiode response trade-off in which the highest photodiode response indicates best part quality.

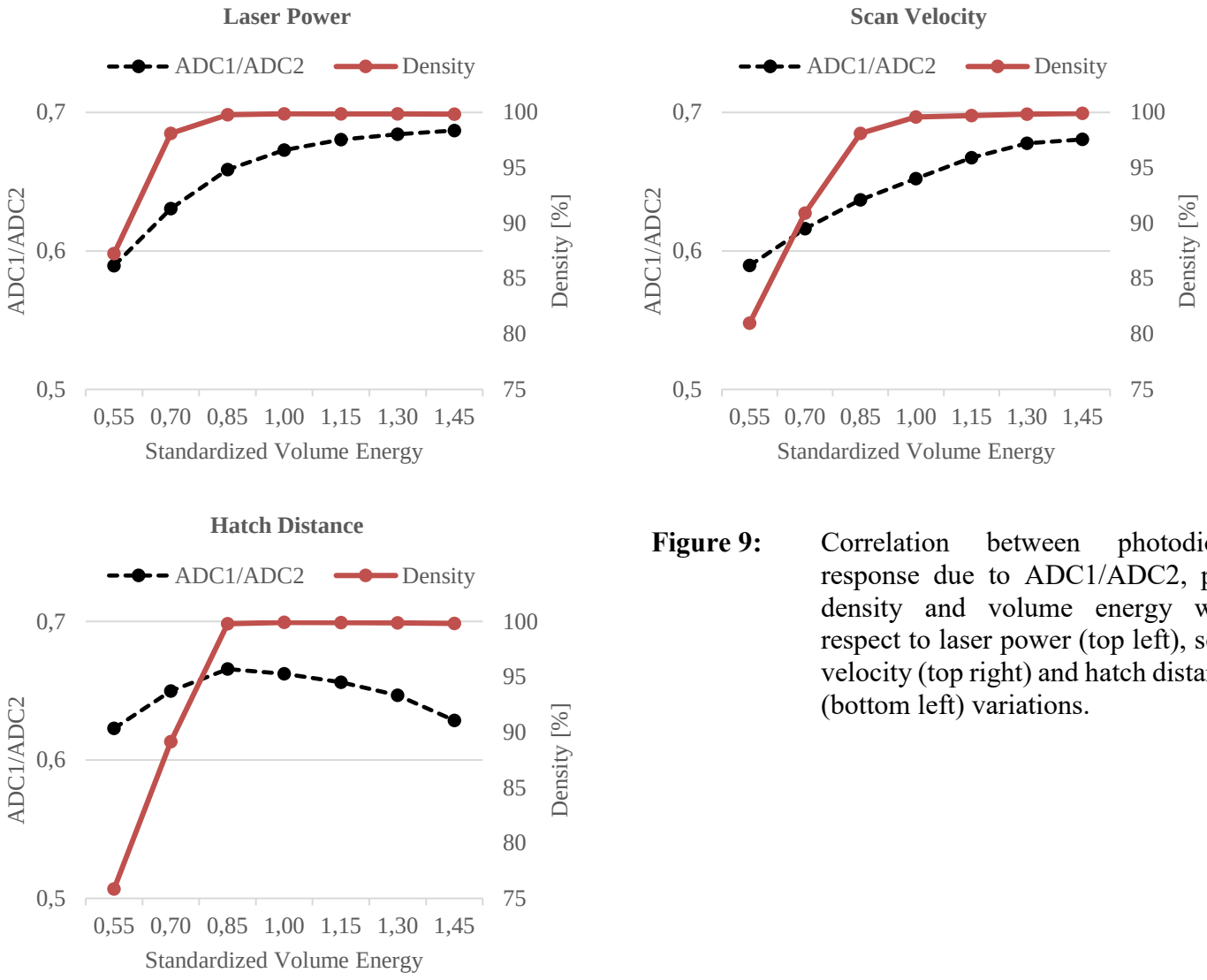

Figure 9: Correlation between photodiode response due to ADC1/ADC2, part density and volume energy with respect to laser power (top left), scan velocity (top right) and hatch distance (bottom left) variations.

Conclusion

The characterization of basis intensity behavior and signal interaction of different process and measurement situations using the real-time melt pool monitoring system from SLM Solutions, based on two different photodiodes, has been performed. The presented single and multiple scan vector approaches could show and indicate the sensitivities of the current monitoring system and enables the transfer of the method for real AM parts. Besides better process understanding these results will lead to further investigations of layer-based and local-based observations.

A general photodiode response was presented by changing wall and volume energy with respect to single and multiple scan vectors via layer thickness, laser power, scan velocity and hatch distance variations. The correlation between parameter change and photodiode response for single scan vectors offers a first and fast basis of interpretation. It is possible to analyze if a certain process parameter or another influencing factor is able to detect as well as usable as a first investigation of the photodiode response resolution due to the parameter variation for the presented melt pool monitoring system.

Finally, this study showed a correlation between part density and photodiode response due to layer thickness, laser power, scan velocity and hatch distance variations, which lead to a volume energy change. Independent and separate analysis of the two photodiodes offer further process understanding and lead to clear process relation behaviors in combination with the quotient of the two photodiodes. The ratio response of

photodiode 1 and photodiode 2 leads to a new quality assurance tool due to global quality diagnostic of density, which has been shown as an offline or post-processing approach. That method can be easily use as an online or in-line quality assurance tool. At that moment, due to photodiode response even a determination of the layer thickness is possible to distinguish to laser power, scan velocity and hatch distance. As widely known, independent from process parameter variation the volume energy has to have a certain critical minimum, which enables the fabrication of almost completely dense parts. In face of current challenges and objectives due to hatch distance variations it has been worked out, that a ratio response >0,66 corresponds to a minimum part density of 99,7 % that meets the demanding requirements of the industry.

Outlook

Future works will concentrate on automatically, online "Global Quality Diagnostic" (GQD) due to any other global quality features like hardness or surface roughness. Within the online approach, there is the possibility to analyze global quality gradients as well as carrying out analyzes during the job. The GQD approach have to expand on various material systems. First results have to be statistically proven that there is the ability to define deviation limits and diagnostic resolutions as well as the documentation of a report. Additional process parameters as well as different machine, material, measurement and environment conditions have to investigate. Furthermore GQD have to show the same performance day-by-day and machine-by-machine being able to use in sensitive and high-class industrialization environment.

A second future focus will lead to "Local Quality Diagnostic". Therefore local part defects and other anomalies as mentioned are carried out with respect to layer-based, single scan or single measuring point analyses.

References

[Alb16] Alberts, D.: Qualitätssicherung beim SLM®-Verfahren - Prozessüberwachung in Hochgeschwindigkeit. 20. Augsburger Seminar für additive Fertigung.

[ASW16] Alberts, D.; Schwarze, D.; Witt, G.: High speed melt pool & laser power monitoring for selective laser melting (SLM®). 9th International Conference on Photonic Technologies LANE 2016. http://lane-conference.org/downloads/IndustrialContributions/LANE2016_1219_Alberts_IC_endformat.pdf.

[BBL10] Berumen, S. et al.: Quality control of laser- and powder bed-based Additive Manufacturing (AM) technologies. In Laser Assisted Net Shape Engineering 6, Proceedings of the LANE 2010, Part 2, 2010, 5, Part B; S. 617–622.

[BSH11] Buchbinder, D. et al.: High Power Selective Laser Melting (HP SLM) of Aluminum Parts. In Physics Procedia, 2011, 12; S. 271–278.

[KAS15] KASPO Maskin AS: Selective Laser Melting at its best. SLM Solutions company presentation 2015. http://hniforum.no/cmsAdmin/uploads/slm-presentasjon-brattv-g.pdf.

[Kra17] Krauss, H.: Qualitätssicherung beim Laserstrahlschmelzen durch schichtweise thermografische In-Process-Überwachung. Utz Verlag GmbH, 2017.

[Kro15] Krol, T. A.: High Batch Repair of Aerospace Components using Selective Laser Melting. RapidTech 2015 Erfurt, 2015.

[KZS12] Kleszczynski, S. et al.: Error detection in laser beam meltingsystems by high resolution imaging. In Proceedings of the Twenty Third Annual International Solid Freeform Fabrication Symposium, 2012, 2012.

[KZS14] Kleszczynski, S.; Zur Jacobsmühlen, J.; Sehrt, J. T., Witt G.: Improving Process Stability of Laser Beam Melting Systems. In Fraunhofer Direct Digital Manufacturing Conference, 2014.

[Nee14] Neef, A.: Low coherence interferometry in selective laser melting, 2014.

[PDS10] Pavlov, M.; Doubenskaia, M.; Smurov, I.: Pyrometric analysis of thermal processes in SLM technology. In Physics Procedia, 2010, 5; S. 523–531.

[RAH13] Rockstroh, T.; Abbott, D.; Hix, K.; Mook, J.: Additive manufacturing at GE Aviation. Lessons learned from development cycle. http://www.industrial-lasers.com/articles/print/volume-28/issue-6/features/additive-manufacturing-at-ge-aviation.html, 07.12.2014.

[Reh10] Rehme, O.: Cellular Design for Laser Freeform Fabrication. Cuvillier, Göttingen, 2010.

[RSB16] Rieder, H. et al.: On- and offline ultrasonic characterization of components built by SLM additive manufacturing. AIP Publishing LLC, 2016; S. 130002.

[Sch14] Schapansky, A.: Reparing parts with additive technologies – An integrated process for measurement, build-up and post-processing. In Proceedings of Rapid.Tech 2014, 2014.

[SG16] Spears, T. G.; Gold, S. A.: In-process sensing in selective laser melting (SLM) additive manufacturing. In Integrating Materials and Manufacturing Innovation, 2016, 5; S. 683.

[SHP16] Smith, R. J. et al.: Spatially resolved acoustic spectroscopy for selective laser melting. In Journal of Materials Processing Technology, 2016, 236; S. 93–102.

[SLM17] SLM Solutions NA INC: SLM 500 Selective Laser Melting System Highlights, 25.05.2017.

[WPH14] Waller, J. M. et al.: Nondestructive Evaluation of Additive Manufacturing State-of-the-Discipline Report. NASA WSTF, 2014.

[WS14] Wiesner, A.; Schwarze, D.: Multi-Laser Selective Laser Melting. LANE 2014 - 8th International Conference on Photonic Technologies. http://lane-conference.org/downloads/IndustrialContributions/LANE2014_Wiesner_Multi-Laser_Selective_Laser.pdf, 5.2016.

[WSP14] Waller, J.; Saulsberry, R.; Parker, B.; Hodges, K.; Burke, E.; Taminger, K. Waller, J. et al.: Summary of NDE of Additive Manufacturing Efforts in NASA, 2014.

[YHC16] Yang, L. et al.: Design for Additively Manufactured Lightweight Structure: A Perspective. In Solid Freeform Fabrication 2016: Proceedings of the 26th Annual Internationa, 2016, 2016.